Quantum materials for spin to charge conversion

Dissertation

zur Erlangung des akademischen Grades

Doktor-Ingenieur (Dr.-Ing.)
der Naturwissenschaftlichen Fakultaet II - Chemie, Physik und Mathematik

der Martin-Luther-Universitaet Halle-Wittenberg

vorgelegt von Herrn
Avanindra Kumar Pandeya

geb. am Muzaffarpur, India

Gutachter: Prof. Dr. Stuart S. P. Parkin

Tag der mündlichen Prüfung:

Zusammenfassung

Abstract

Acknowledgements

The last few years would not have been as interesting and enjoyable without the help and the company of certain special people. Primarily, I am very grateful to Prof. Parkin for a very inspiring time and the chance to work on a lot of interesting projects. I have learned a lot from you and I very much enjoy discussing physics with you. Thank you for always supporting me and for giving me many valuable opportunities throughout my PhD. I want to thank Amilcar Bedoya Pinto for being the first one to get me interested in this exciting field of physics. You have supported me in many different ways throughout my years at the university and I am very grateful for that.

I have profited a lot from discussing and doing physics with many great people I have met during the last years. Special thanks go to my fellow PhD students... for uncounted hours of interesting and very helpful discussions. Further thanks for invaluable discussions go to . Particular thanks also goes to friends and colleagues I have met throughout the years: . It would not have been the same without you. A huge thank you goes to ... for many memorable experiences throughout the last nine years. Last, extraordinary thanks go to my family for always supporting me!

Contents

The story so far: In the beginning the Universe was created. This has made a lot of people very angry and been widely regarded as a bad move.

Douglas Adams

1

Introduction

1.1 Moore's Law – Room at the bottom is shrinking

The number of transistors per unit area in electronic circuit keeps doubling almost every two years. It was first observed by Gordon Moore in his 1965 paper. In many ways Moore's law has been surpassed so far. Aggressive scaling of electronic devices which has followed Moore's law has made "plenty of room" for storage and devices as Feynman had once envisaged in his famous lecture. But pace of growth is plateauing and the there is a limit to where CMOS can take us.

Memory devices has similarly experienced a lot of growth dues to scaling but we are reaching the limits of what can be achieved. The main form in which data is stored is magnetic bits and these bits are read and written using magnetic read/write head.

1.2 Spintronics for scaling and beyond

1.3 Quantum materials for spintronics

1.4 Dichalcogenides

1.5 Weyl semi-metals

1.6 Outline

2

Spintronics and Quantum Materials

2.1 Spin current - Two current model

At a very basic level, spin current if net transfer of spins from one point to another. Spin Current is actually defined as a tensor $q_i j$, where i denotes the direction of flow of spin current and j denotes the which component of spin is flowing[7]. The indices i and j are the directions in the 3D space. We can, in principle, have an net spin current without any flow of charge current, if equal amount of up and down electron are moving in opposite direction. That is why these are often touted as dissipationless[8]. But in reality, one always needs some amount of charge current to create the spin current in the first place which should be taken into consideration for making a fair comparison.

There can be a net spin current if there is an imbalance between the up spin and down spin flowing in the opposite direction to each other. Let us define electrical spin polarization P_j in the direction j as follows:

$$P_j = \frac{n^{\uparrow} - n^{\downarrow}}{n^{\uparrow} + n^{\downarrow}} \tag{2.1}$$

??

2.2 How to create spin current?

We can create spin current using many methods. One of the most simple methods is to take a ferromagnet and pass current through it and inject the

current coming out of the ferromagnet into wherever we might need[9]. But this is a fairly inefficient method. There are other methods like spin pumping, spin Hall effect and inverse spin galvanic effect (Rashba-Edelstein effect) etc. Let us discuss these methods in detail.

2.3 How to measure spin current?

2.4 Landu-Lifshitz-Gilbert Equation

The magnetization of a sample experiences a torque perpendicular to the direction of applied field and the direction of magnetization. In absence of any damping the magnetization can keep precessing around the applied field forever. But in real materials the radius of precession keeps decreasing and eventually all the magnetizations point towards the applied magnetic field.

$$\dot{\mathbf{M}} = -\gamma(\mathbf{M} \times \mathbf{H}) + \frac{\alpha}{M}\left(\mathbf{M} \times \dot{\mathbf{M}})\right) \tag{2.2}$$

2.5 Spin-Torque Ferrmomagnetic Resonance - STFMR

When a dc magnetic field H_{ext} is sweeped in the STFMR configuration, the mixing voltage [10], can be expressed as in **??**:

$$V_{mix} = V_0 + V_{sym}\frac{\Delta H^2}{\Delta H^2 + (H_{ext}^2 + H_{res}^2)} + V_{as}\frac{\Delta H\,(H_{ext} - H_{res})}{\Delta H^2 + (H_{ext}^2 + H_{res}^2)} \tag{2.3}$$

We fit this equation to extract fitting parameters V_0, H_{res}, V_{sym}, V_{as}, H_{res}, and Δ. When there is no DC current passing through the metal layer, the resonance field can be used to fit effective magnetization using Kittel formula [11] using **??**.

$$f_{res} = \frac{\gamma}{4\pi}\sqrt{(H_{res} + H_0)(H_{res} + H_0 + M_{eff})} \tag{2.4}$$

The Gilbert damping can be extracted from the linewidth of the resonance peak [11] using equation **??**.

$$\Delta H = \Delta H_{res} + \frac{2\pi f}{\lambda}\alpha \tag{2.5}$$

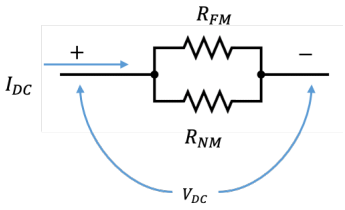

Fig. 2.1: Parallel connection between the ferromagnetic and normal metal layer

When a dc current is passed through the normal metal it pumps spin current into the ferromagnetic layer. In presence of a spin current the equation (4) is modified as [12], [13]:

$$\Delta H = \Delta H_{res} + \frac{2\pi f}{\lambda}\left(\alpha + \frac{\sin\phi}{(H_{ext} + 0.5M_{eff})\mu_0 M_s t}\frac{\hbar}{2e}J_s\right) \tag{2.6}$$

The change in linewidth ($\delta\Delta H$) for two different values of spin current ($\Delta J_s = J_{s1} - J_{s2}$) will be:

$$\delta\Delta H = \frac{2\pi f}{\lambda}\left(\alpha + \frac{\sin\phi}{(H_{ext} + 0.5M_{eff})\mu_0 M_s t}\frac{\hbar}{2e}J_s\right) \tag{2.7}$$

The **??** can be rearranged to get an expression of ΔJ_s:

$$\Delta J_s = \frac{\delta\Delta H}{\frac{2\pi f}{\lambda}\left(\alpha + \frac{\sin\phi}{(H_{ext}+0.5M_{eff})\mu_0 M_s t}\frac{\hbar}{2e}J_s\right)} \tag{2.8}$$

We can assume a simple model of parallel connection between the ferromagnetic layer and the normal metal layer to find out the current distribution within the bilayer.

The current density through the metal layer is calculated as follows:

$$J_{NM} = \frac{I_{NM}}{A_c} = \frac{V_{DC}/R_{NM}}{A_C} = I_{DC}\frac{R_{FM}R_{NM}}{R_{FM}+R_{NM}}\frac{1}{R_{NM}A_C} \tag{2.9}$$

$$\implies J_{NM} = I_{DC}\frac{R_{FM}}{(R_{FM}+R_{NM})A_C} \tag{2.10}$$

$$\implies \Delta J_{NM} = \Delta I_{DC} \frac{R_{FM}}{(R_{FM} + R_{NM}) A_C} \tag{2.11}$$

Using **??** and **??** , we have

$$\theta = \frac{\Delta J_{NM}}{\Delta J_S} \tag{2.12}$$

$$\implies \theta = \frac{\delta \Delta I_H / \delta \Delta I_{DC}}{\frac{2\pi f}{\lambda} \left(\alpha + \frac{\sin \phi}{(H_{ext} + 0.5 M_{eff}) \mu_0 M_s t} \frac{\hbar}{2e} J_s \right)} \frac{R_{FM}}{(R_{FM} + R_{NM})} A_C \tag{2.13}$$

This is the final relation which we use to calculate the Spin-Hall ratio in our experiments.

2.6 Second Harmonic Hall

Let us take a hall bar of NM-FM heterostructure and pass ac current ($I_0 \sin \omega t$) through it in presence of an in-plane magnetic field (B_0) and measure transversal voltage ($V_{xy}(t)$) across it. The effective magnetic field acting on the sample will have both ac and dc components:

$$\mathbf{B} = \mathbf{B_{DC}} + \mathbf{B_{ac}(t)} \tag{2.14}$$

where,

$$\mathbf{B_{DC}} = \mathbf{B_0} + \mathbf{B_{ani}} \tag{2.15}$$

$$\mathbf{B_{ac(t)}} = \mathbf{B_{AD}} + \mathbf{B_{FL}} + \mathbf{B_{Oe}} = \mathbf{b} \sin \omega t \tag{2.16}$$

$$V_{xy}(t) = R_{xy}(t) \times I_0 \sin \omega t \tag{2.17}$$

$$R_{xy}(t) = R_{xy}\left(\mathbf{B_{DC}}\right) + \frac{\partial R_{xy}}{\partial \mathbf{B_{ac}}}\mathbf{b}\sin\omega t \tag{2.18}$$

$$V_{xy}(t) = \left(R_{xy}\left(\mathbf{B_{DC}}\right) + \frac{\partial R_{xy}}{\partial \mathbf{B_{ac}}}\mathbf{b}\sin\omega t\right) I_0 \sin\omega t \tag{2.19}$$

$$V_{xy}(t) = R_{xy}\left(\mathbf{B_{DC}}\right) I_0 \sin\omega t + \frac{\partial R_{xy}}{\partial \mathbf{B_{ac}}} I_0 \mathbf{b}\sin^2\omega t \tag{2.20}$$

$$V_{xy}(t) = R_{xy}\left(\mathbf{B_{DC}}\right) I_0 \sin\omega t + \frac{\partial R_{xy}}{\partial \mathbf{B_{ac}}} I_0 \mathbf{b}\left(\frac{1-\cos 2\omega t}{2}\right) \tag{2.21}$$

$$V_{xy}(t) = R_{xy}\left(\mathbf{B_{DC}}\right) I_0 \sin\omega t + \frac{1}{2}\frac{\partial R_{xy}}{\partial \mathbf{B_{ac}}} I_0 \mathbf{b} - \frac{1}{2}\frac{\partial R_{xy}}{\partial \mathbf{B_{ac}}} I_0 \mathbf{b}\cos 2\omega t \tag{2.22}$$

$$V_{xy}(t) = R^0_{xy} I_0 + R^{\omega}_{xy} I_0 + R^{2\omega}_{xy} I_0 \tag{2.23}$$

Comparing **??** and **??**, we get:

$$R^0_{xy} = \frac{1}{2}\frac{\partial R_{xy}}{\partial \mathbf{B_{ac}}}\mathbf{b} \tag{2.24}$$

$$R^{\omega}_{xy} = R_{xy}\left(\mathbf{B_{DC}}\right)\sin\omega t \tag{2.25}$$

$$R^{2\omega}_{xy} = -\frac{1}{2}\frac{\partial R_{xy}}{\partial \mathbf{B_{ac}}}\mathbf{b}\cos 2\omega t \tag{2.26}$$

This means that the first harmonic amplitude is exactly like the Dc measurement which will have AHE and PHE effect contributions[14]:

The second harmonic signal has three major source contributions:

1. Contribution due to Oerested Field

2. Contribution due to torque on the magnetization of FM due to the spin current from the NM

3. ontribution due to the thermal gradient along the substrate to the top layer of the film

The second harmonic expression for transverse resistance can be written as:

$$\begin{aligned} R_{xy}^{2\omega} &= (R_{AHE} - 2R_{PHE}\cos\theta\sin 2\phi)\frac{\partial\cos\theta}{\partial\theta_B}\frac{B_{ac}^{\theta}}{B_0\cos(\theta_B-\theta)} \\ &\quad + R_{PHE}\sin^2\theta\frac{\partial\sin 2\phi}{\partial\phi_B}\frac{B_{ac}^{\phi}}{\sin\theta_B\sin(\theta_B-\theta)B_0} \\ &\quad + \alpha\nabla T I_0\sin\theta\cos\phi \end{aligned} \tag{2.27}$$

When the field is applied in-plane of the sample $\theta_B = \pi/2$ and for permalloy with PMA, $\theta \approx \pi/2$, and $\phi_B \approx \phi$ above equation can be simplified to:

$$R_{xy}^{2\omega} = R_{AHE}\frac{\partial\cos\theta}{\partial\theta_B}\frac{B_{ac}^{\theta}}{B_0} + R_{PHE}\frac{\partial\sin 2\phi}{\partial\phi_B}\frac{B_{ac}^{\theta}}{B_0} + \alpha\nabla T I_0\sin\theta\cos\phi \tag{2.28}$$

Calculating the derivatives at the above mentioned angles, we get,

$$R_{AHE}\frac{\partial\cos\theta}{\partial\theta_B} = R_{AHE}\sin\theta\partial\theta\theta_B = R_{AHE} \tag{2.29}$$

$$R_{PHE}\frac{\partial\sin 2\phi}{\partial\phi_B} = R_{PHE}2\cos 2\phi = R_{PHE}\left(\cos^2\phi - 1\right) \tag{2.30}$$

Substituting these values from **??** and **??** into **??** we get,

$$R_{xy}^{2\omega} = R_{AHE}\frac{B_{ac}^{\theta}}{B_0} + R_{PHE}\left(\cos^2\phi - 1\right)\frac{B_{ac}^{\phi}}{B_0} + \alpha\nabla T I_0\sin\theta\cos\phi \tag{2.31}$$

The antidumping and field like torques are given by:

$$\mathbf{B_{AD}} = B_{AD}\left(\mathbf{m}\times\mathbf{y}\right) = B_{AD}\cos\phi\ \hat{\theta} \tag{2.32}$$

$$\mathbf{B_{FL+Oe}} = (B_{FL} + B_{Oe})\,(\mathbf{m} \times \mathbf{m} \times \mathbf{y}) = (B_{FL} + B_{Oe}) \cos\phi\ \hat{\phi} \tag{2.33}$$

Substituting these values from **??** and **??** in the expression for second harmonic resistance in **??** we get,

$$R_{xy}^{2\omega} = R_{AHE}\frac{B_{AD}\cos\phi}{B_0} + R_{PHE}\left(\cos^2\phi - 1\right)\frac{(B_{FL} + B_{Oe})}{B_0} + \alpha\nabla T I_0 \sin\theta\cos\phi \tag{2.34}$$

$$R_{xy}^{2\omega} = \left[\left(R_{AHE}\frac{B_{AD}}{B_0} + \alpha\nabla T I_0\right)\cos\phi + 2R_{PHE}\left(\cos^3\phi - \cos\phi\right)\frac{(B_{FL} + B_{Oe})}{B_0}\right] \tag{2.35}$$

The simulation of the above equation gives following result.

The raw data is symmetrized before fitting to get rid of unwanted contrinutions due to misalignement of Hall branches, or misalignment of sample with respect to external fields. The odd part of the second harmonic signal and the even part of the first harmonic signal is take before fitting the data.

2.7 final

3

Experimental Set Up

3.1 PAPAYA - Multi-purpose chamber for production and analysis of nano-systems

PAPAYA is growth-cum-analysis chamber which allows users to grow samples using MBE and characterize them using various in-situ techniques. It has 3 MBE chambers, an XPS chamber and a low temperature STM-cum-Q plus AFM. The system have following features:

1. Selenide MBE : We can grow various Metal Selenide in this chamber. It's one port has Se and has 4 ports for other metals like Nb, Pd, V etc. The substrate can rotate up to 320°C and heated up to 900°C The chamber has RHEED for characterizing the thin film while growing it.

2. Telluride MBE: Various Tellurides can be grown in this chamber. It has only 3 ports and has mateials like SnTe in it. It has not been used in this work and hence, will not be described in detail here.

3. Metal MBE: Despite its name we can grow both metals and non-metals in it. It has 5 ports and Al, MgO, Py (Ni80Fe20), Ni and Cu can be grown in this chamber. The sample can rotated for 360°C but can be heated and hence, everything is grown at room temperature.

4. In-Situ X-ray photoelectron spectra (XPS) system: XPS is a surface sensitive techinique which can be used to characterize the elemental composition

of a material and chemical states of these elements. It is a standard characterization tool based of photoelectric effect. When X-Ray with energy (E_{photon}) with falls on a material with electron withbinding energy ($E_{binding}$) and surface work function (ϕ), electrons with energy ($E_{kinetic}$) are emitted.

$$E_{binding} = E_{photon} - (E_{kinetic} + \phi) \tag{3.1}$$

The kinetic energy of the emitted electrons is measured using a hemispherical analyser and using the **??** we can estimate the binding energy of the electrons. The XPS spectrum is number of detected electrons as a function of binding (or kinetic energy). A peak is observed corresponding to the binding energies of the electrons present in an element. Every element has electrons at fixed binding energies and thus, a set of peaks can serve as a fingerprint of the element. The position of the peaks may increase or decrease by a little bit based on its chemical state. The relative concentration of various elements can be estimated by taking the ratio of area under the curve of these peaks after taking relative sensitivity factor into account and subtracting background properly.

$$\frac{C_1}{C_2} = \frac{A_1 \times r_2}{A_2 \times r_1} \tag{3.2}$$

An omicron machine with Al and Mg sources is attached to PAPAYA. The measurements can be done only at room temperature in this system.

5. In-Situ Scanning Tunneling Microscope (STM): The STM experiments were performed on an Omicron VT-STM-XT system operated at room temperature with a base pressure of 2×10^{-11} mbar. The mechanically sharpened Pt/Ir tips were treated and checked on Au(111) surface before measurements, and the topography images were acquired at room-temperature.

3.2 TAMARIND - Topological materials engineering by epitaxial design

It can be used to phosphides and arsenides. It has 7 ports in which Nb, Ta, Py, MgO, GaP (as source of P) and GaAs (as source of As) is attached. The

substrate can be rotated up to 320 and heated up to 1200 C using resistive heating. To achieve higher substrate temperature there is a possibility to use e-beam heating. The substrate can be cooled using liquid N2 to up to -30 C. There is a RHEED to monitor the growth of the film. There is a residual gas analyser and a mass spectrometer to monitor the partial pressure of various gaseous species in the chamber.

3.3 STFMR Set-Up

3.4 Second Harmonic Hall Set Up

4

Growth and Structural Characterization of Quantum Materials

4.1 Growth of $NbSe_2$

$NbSe_2$was grown using Molecular beam epitaxy (MBE) on c-plane of sapphire substrate from Crystec. The substrate was cleaned using modified RCA method as described in **??** and loaded in the selenide chamber of PAPAYA where it was degassed at 700°C for about 1 hour. Nb and Se are co evaoparoated from e-beam and K-cells respectively such that ther flx ratio is 1:20. The first 3 monolayers (MLs) were grown at 570°C and all the subsequent layers were grown at 650°C. The deposited sample was annealed at 700°C for the first time after deposition of 3 ML and then intermittently after every 10-15 MLs. The growth is monitored continuously using RHEED and the the stoichiometry and morphology is assessed intermittently using XPS and STM respectively. Once the sample is taken out of the chamber its structure is assessed using XRD and Raman.

4.1.1 Cleaning Al_2O_3substrate

The substrates which we recieve from the suppliers usually have both metallic and organic impurities on them. The AFM of the substrate as recieved from the supplier is shown in **??** The recipe for cleaning the substrate is as follows:

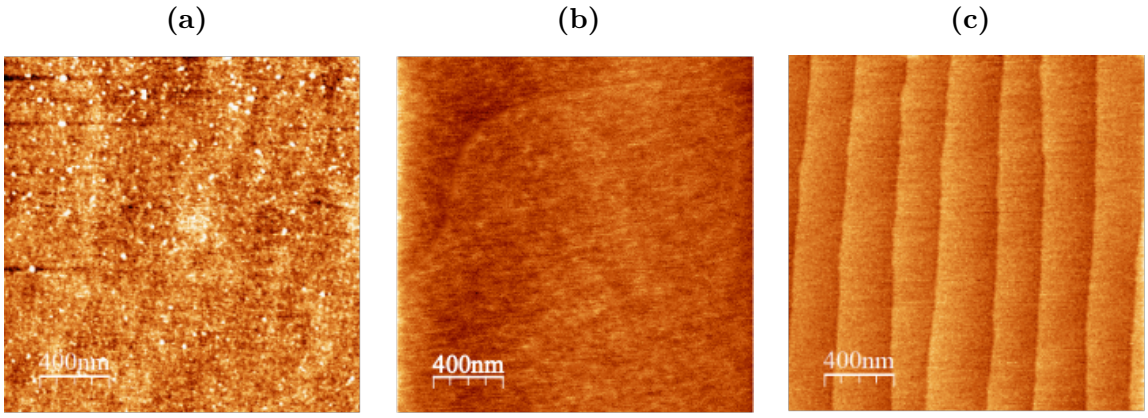

Fig. 4.1: AFM image of Al2O3 sunstrates **(a)** as received form Crystec, **(b)** after modified RCA cleaning of the substrate, and **(c)** after annealing of the cleaned before loading in growth chamber. The chemical cleaning helps in removing all the impurities on the substrate.

1. Soak the substrate in ethanol for 12 hours.
2. Clean the substrate in ultrasonic bath of acetone and Isopropanol for 5 minutes each to remove bulky dissolvable contaminants and particulates materials.
3. Rinse thoroughly in deionized (DI) water thoroughly and blow with dry nitrogen gas.
4. Heat the substrate in $NH_4OH : H_2O_2 : H_2O = 1 : 1 : 5$ to about $80^{\circ}C$ for 10 minutes NH^{4+}in the cleaning solution will complex with heavy metal on the substrate surface to form a soluble metal salts which is removed.
5. Rinse thoroughly in DI water thoroughly and dry with pure nitrogen gas.
6. Soak the substrate in solution of $HCl : H_2O_2 : H_2O = 1: 1: 3$ at about $80^{\circ}C$ for 10 minutes H^+ ion in the cleaning solution will replace with the light metal impurities to form soluble salt and be removed.
7. Rinse thoroughly in DI water thoroughly and dry with pure nitrogen gas.
8. Clean in $H_2SO_4 : H_3PO_4 = 1 : 3$ at about $80^{\circ}C$ for 10min to move the oxide layer on the sapphire substrate
9. Rinse thoroughly in DI water thoroughly and dry with pure nitrogen gas.

10. After drying the sapphire substrate anneal at 1200°C for 4h preferably, but not necessarily, in the O_2 atmosphere.

We are able to get rid of the impurities after chemically cleaning it as can be seen in **??**. The terraces of the substrate are visible in **??** after annealing it in O_2 atmosphere. The width of the terraces is dependent on the miscut angle of the substrate. Lower the miscut angle, wider the terraces. The cleaned substrate was then loaded into the selenide chamber of PAPAYA where it was first degassed at 700°C for about 1 hour. The substrate surface is now ready for growth of $NbSe_2$.

The growth of any thin film using MBE can be affected by two major factors:

1. temperature of the substrate and
2. flux ratio of the elements of the film

I will discuss their effect on growth of NbSe2 film one by one.

4.1.2 Temperature of the substrate

A two-step growth method gives us more crystalline NbSe2. 99.999% pure Nb was evaporated using an e-beam cell and Se was evaporated using K-cell with a flux ratio >1:20. The first 3 monolayer (ML) is grown at 570 ± 20 10°C and all the subsequent layers are grown at 650 ± 20 10°C . The deposited sample is annealed at 700 ± 20 10°C for the first time after deposition of 3 ML and then intermittently after every 10-15 ML.

Long streaky RHEED patterns of the (0001) Al2O3 in $[10\bar{1}0]$ and $[11\bar{2}0]$ directions were observed indicating a flat and crystalline substrate surface (**??** and **??**). As the growth of forst monolayer completes the RHEED appears a bit diffused(**??** and **??**) but as the growth progresses the patter becomse streakier (**??** and **??**).It means that the grain size increases as the film grows thicker because of increased coalescence. Using RHEED, the in-plane lattice parameter for this film is estimated to be 3.46 ± 0.03 Å.

We characterized the sample using X-Ray diffraction (XRD) and Raman Spectroscopy after taking it out of the growth chamber.

4.2 Growth of Weyl Semimetals

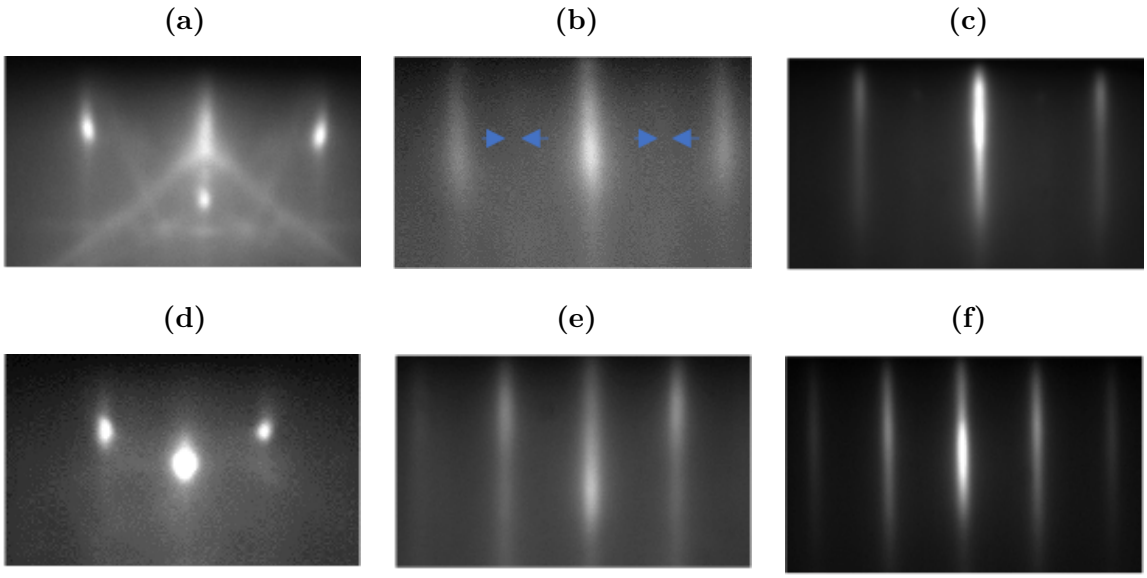

Fig. 4.2: The evolution of RHEED image of $[10\bar{1}0]$ direction of **(a)** substrate: Al_2O_3, **(b)** interfacial layer of $NbSe_2$ and, **(c)** $NbSe_2$ after 6h growth. After rotating the sample by 30°, we observe $[11\bar{2}0]$ direction of **(d)** substrate , **(e)** interfacial $NbSe_2$, **(f)** $NbSe_2$ after 6h growth.